



Optimal use of glycerol co-solvent to enhance product yield and its quality from hydrothermal liquefaction of refuse-derived fuel

S. Harisankar¹ · P. Francis Prashanth¹ · Jeganathan Nallasivam¹ · R. Vinu¹

Received: 22 January 2022 / Revised: 5 May 2022 / Accepted: 6 May 2022 / Published online: 23 May 2022
© The Author(s), under exclusive licence to Springer-Verlag GmbH Germany, part of Springer Nature 2022

Abstract

Refuse-derived fuels (RDF) are rich in resources that make them an attractive feedstock for the production of energy and biofuels. Hydrothermal liquefaction (HTL) is a promising thermochemical conversion technology to handle wet feedstocks and convert them to valuable bio-crude, bio-char and aqueous products. This study highlights the advantages of using glycerol as the co-solvent along with water in different proportions to produce bio-crude from RDF via HTL. The ratio of water:glycerol (vol.%,vol.%) was varied for each experiment (100:0, 90:10, 80:20, 70:30, 60:40, 50:50), and the product yields and their quality were studied. The results demonstrate that increasing the proportion of glycerol until 50 vol.% in the solvent enhances the bio-crude yield (36.2 wt.%) and its higher heating value (HHV) (30.9 MJ kg⁻¹). Deoxygenation achieved in the bio-crude was 42%. The production of bio-char was minimum (9.5 wt.%) at 50 vol.% glycerol with HHV of 31.9 MJ kg⁻¹. The selectivity to phenolic compounds in the bio-crude increased, while that of cyclic oxygenates decreased when the glycerol content was more than 20 vol.%. The gas-phase analysis revealed that the major deoxygenation pathway was decarboxylation. The yield of aqueous products drastically increased with the addition of glycerol. The minimum amount of glycerol in the co-solvent that favours an energetically feasible process with low carbon footprint is 30 vol.%. Using 50 vol.% glycerol resulted in the highest energy recovery in the bio-crude and bio-char (80%), the lowest energy consumption ratio (0.43) and lowest environmental factor (0.1). The mass-based process mass intensity factor, calculated based on only bio-crude and bio-char as the valuable products, decreased with an increase in addition of glycerol, while it was close to unity when the aqueous phase is also considered as a valuable product.

Keywords Hydrothermal liquefaction · Refuse-derived fuel · Glycerol · Bio-crude · Energy recovery · Co-solvent

1 Introduction

Due to rapid industrialisation and urbanisation, humankind has left a huge amount of wastes behind, and the consequences of leaving these without treatment are alarming. It is estimated that at least 14 million tonnes of trash make their way into the oceans and kill nearly a million marine creatures every year [1]. Every year, in a developing country like India, 62 million tonnes of municipal solid wastes (MSW) are generated, out of which only 11.9 million tonnes are treated, 31 million tonnes are dumped in landfills and the remaining are left uncollected [2]. MSW is the primary

source of refuse-derived fuel (RDF). RDF is obtained from MSW after mechanical segregation process to separate the decaying matter (food waste, animal waste) and non-combustible materials such as metals and glass from the non-biodegradable matter. The segregated decaying matter is used for composting, while the metals and glass are generally recycled. On an average, 20% of the Indian MSW can be considered the RDF fraction, and at least 28,000 tons of RDF is available per day for co-processing in cement plants [3]. The major constituents of RDF are plastics (22–56 wt.%), paper (46–58 wt.%), wood (2.3–62 wt.%), textile wastes (3.1–15 wt.%) and inert matter (~8.5 wt.%) [4]. The wide variation in the composition of RDF is mainly due to the differences in the economic status and lifestyle of the people. Even though RDF is extremely heterogeneous, it is a source of valuable chemicals, energy and bio-products. Therefore, developing an eco-friendly process that can recover energy and value from RDF is essential for a sustainable future.

✉ R. Vinu
vinu@iitm.ac.in

¹ Department of Chemical Engineering and National Center for Combustion Research and Development, Indian Institute of Technology Madras, Chennai 600036, India

Hydrothermal liquefaction (HTL) is a thermochemical conversion process, which utilises water at near-critical conditions to process any carbonaceous feedstock such as lignocellulosic biomass, MSW, macroalgae, microalgae and RDF, and converts them to bio-crude and bio-char. Around its critical point (374 °C and 22.1 MPa), water acquires properties similar to an organic solvent with lower density ($\sim 0.6 \text{ g cm}^{-3}$) and dielectric constant (~ 10) [5]. Owing to an enhanced ionic constant at these conditions, it catalyses a variety of redox reactions. The major advantage of HTL is that it can process wet feedstocks with moisture content as high as 80%. In a way, the process mimics the geological formation of crude oil, but with a handful of operating conditions to tailor-make the product yields and their quality.

Several studies have shown that the product yields from liquefaction of biomass vary with the operating conditions, of which temperature and catalysts are the major factors [6]. The composition of the feedstock [7] and pH of the reaction mixture [8] are two other factors that also affect the yield and quality of products from HTL. It was found that the presence of co-solvents like glycerol, ethanol and alkaline catalysts like CaCO_3 , Na_2SO_4 , KOH and Na_2CO_3 highly influence the yield and the product characteristics [9, 10]. Oxygen heteroatom is removed from organic compounds via dehydration and decarboxylation, while nitrogen is removed by deamination reactions [11]. Since water is fully oxidised and has no residual heating value, it is possible to remove oxygen without losing heating value in the aqueous medium [5]. Hence, the ratio of (H+C):O of the HTL bio-crude is higher than that of pyrolysis bio-oil, which eventually results in better energy density and heating value of the HTL bio-crude.

A major problem associated with bio-crude is its high viscosity, typically of the order of 10^4 cP (at 60 °C) [12]. Various interactions occur among the different macromolecules during co-liquefaction of biomass with wastes, which significantly affect the yield and quality of the products [13]. The yield and quality of the bio-crude can be substantially improved by co-liquefaction of biomass with plastics. The higher hydrogen content in plastics is shown to significantly influence the transformation pathways of carbohydrates in the biomass via Maillard reactions of carbohydrates with proteins or amino acids [14]. The enormous generation and disposal of used face masks in the last few years have also raised serious environmental concerns. Co-liquefaction of biomass with face masks at 300 °C is reported to increase the diesel fraction ($\text{C}_{16}\text{--}\text{C}_{21}$) and decrease the heavy fractions ($\text{C}_{25}\text{--}\text{C}_{42}$) in the bio-crude [15]. Wastes such as plastics and face masks are inherently present in RDF and contribute to the high hydrogen content in the feedstock. Hence, the use of RDF as a feedstock in the HTL process could result in an improved quality of the bio-crude.

Solvents with a high self-ionisation constant, higher density, higher dipole moment and lower dielectric constant

than water result in better fragmentation of the feedstock [5]. Moreover, the use of organic solvent in HTL reduces the density and viscosity of the bio-crude [16]. While co-solvents significantly enhance the yield and quality of the products, they also increase the cost of operation. Optimising the use of solvents while maximising the yield and quality of the products at a minimal cost is vital to sustainable operation. Amid the COVID-19 crisis, the global glycerol market is estimated at 2.6 billion USD in 2022, and is expected to grow at a compound annual growth rate of over 6%. Of the total glycerol produced worldwide, more than 10% belongs to the glycerol from the biodiesel industry, i.e. the supply of crude glycerol is higher than its demand due to the advancement in the biodiesel industry [17]. Therefore, using glycerol as a co-solvent in HTL is an attractive proposition.

Several solid waste management regulations around the globe emphasise the valorisation of MSW from old and existing landfills [18]. In developing countries like India, the organic fraction of the MSW is segregated and digested anaerobically to produce compost and biogas, whereas the bio-inorganic fraction from the old landfills remains intact for many years. These are sold as RDF by the municipalities and corporations. The RDF has superior fuel properties as compared to raw MSW due to the presence of high volatile matter and absence of wet biodegradable matter in it. RDF is generally used as secondary fuels, and as an alternative to conventional fossil fuels in cement kilns, incinerators and boilers. However, combustion of RDF has many disadvantages such as low efficiency and harmful emissions such as dioxins, furans and corrosive acid vapours like HCl [19]. HTL of RDF is considered a cleaner and promising valorisation route that can address these limitations. This is due to the feedstock-agnostic nature of the HTL technology. HTL of real, heterogeneous and co-mingled RDF is scarcely explored in the literature. In urban RDF, cellulose is found in the form of paper, cardboard, food waste and garden waste. Lignocellulosic biomass present in the RDF is the primary source of hemicellulose and lignin. Lipids and proteins present in animal wastes and food wastes are usually segregated from MSW for composting before the preparation of RDF.

The heterogeneity of RDF is space and time dependent. An RDF of Portugal origin contained very high volatile matter (85.1 wt.%) and low ash content (10.7 wt.%), with an HHV of 21.2 MJ kg^{-1} [20]. Another sample of RDF of UK origin contained higher ash (26 wt.%) with an HHV of 18.7 MJ kg^{-1} [21]. While literature is available on individual feedstock and simulated waste mixtures, the behaviour of real wastes in the presence of co-solvents under hydrothermal conditions is not widely studied. In this work, for the first time, HTL of an RDF, obtained after the sorting of unsegregated MSW of Indian origin, is carried out in a batch reactor. The effects of varying

glycerol concentration in the solvent medium on product yields and composition have been studied. This is important from the viewpoint of utilising an optimum amount of solvent, which directly impacts the economics of the process. The study aims to obtain fundamental information pertaining to the effect of glycerol co-solvent on the yields and quality of the liquefaction products from real RDF waste streams. Detailed analysis of the product phases, mainly bio-crude and aqueous phase, and the energetic feasibility of the process have been carried out in this study.

2 Experimental section

2.1 Feedstock characterisation

The feedstock for the experiment (RDF) was obtained from the MSW sorting centre in Vengadamangalam (12.8297° N, 80.1401° E) in the Kancheepuram district near Chennai. Size-based segregation of biodegradable and non-biodegradable fractions of MSW was performed using a train of process equipments including shredders, vibratory and trommel screens. Eddy current-based separator and manual labour were also employed to segregate the metal and glass particles. Visual appearance indicated that the RDF contained a significant amount of cloth waste, garden waste and paper along with plastics and inert particles. The bulk RDF samples obtained from different batches were initially hand cut to a 1 to 2-cm size range. This fraction also contained biomass particles smaller than 0.5 cm. After performing size reduction of the samples from different fractions, they were mixed thoroughly to achieve maximum homogeneity.

The feedstock was characterised using an elemental analyser (Thermo Flash 2000, Thermo Fischer Scientific) according to ASTM D-3177, ASTM D-3178 and ASTM D-3179 methods to determine the elemental composition. The proximate analysis was carried out in a thermogravimetric analyser (TGA-2000A, Navas Instruments) according to the ASTM E1131-08 method. In order to carry out the characterisation of RDF, size reduction was further performed to reduce the size of the particles to < 1 mm, and the analyses were performed multiple times to ensure reasonable standard deviation. Table 1 shows the characteristics of the RDF. The RDF had a high amount of volatile matter owing to the presence of plastics. It also had a significant amount of inorganic ash. The high standard deviation on the carbon content signifies the heterogeneity of the sample. Based on the calorific value, the RDF used in this study can be classified as ‘Grade-II’, according to

Table 1 Properties of RDF

Elemental analysis (wt.% dry basis)	Carbon	40.4 ± 5
	Hydrogen	4.6 ± 0.3
	Nitrogen	1.1 ± 0.5
	Sulphur	0.3 ± 0.3
	Oxygen*	18.1
Proximate analysis (wt.% dry basis)	Volatiles	60.5 ± 0.9
	Fixed carbon	4 ± 0.8
	Ash	35.5 ± 0.1
HHV (MJ kg ⁻¹)		16.8

$$*O = 100 - (\%C + \%H + \%N + \%S + \%Ash)$$

the Ministry of Housing and Urban Affairs of the Government of India [3].

2.2 HTL experiments

The experimental setup used to conduct HTL reactions consisted of a batch stainless steel reactor (SS-304) with a capacity of 1.3 L. A band heater was wrapped around the reactor vessel, and a K-type thermocouple connected to a temperature controller was placed inside the thermo-well attached to the reactor head. The reactor lid was fitted with a pressure gauge and a magnetic stirrer. In a typical experiment, 35 g of RDF was loaded with 350 mL of the solvent (feed:solvent ratio of 1:10 w/v) and pressurised to an initial pressure of 1.5 MPa using N₂. It was further heated to 350 °C to reach a final pressure of 20 MPa. The speed of the magnetic stirrer was set at 400 rpm, and the reaction mixture was maintained at the final condition for 30 min. More details regarding the experimental setup are available in our previous reports [22, 23]. The ratio of water:glycerol (vol.%:vol.%) was varied as 100:0 (Experiment A1), 90:10 (Experiment A2), 80:20 (Experiment A3), 70:30 (Experiment A4), 60:40 (Experiment A5) and 50:50 (Experiment A6).

After holding the reaction mixture at the operating condition for 30 min, the reactor was allowed to cool down. The gases were collected through the pressure release valve in Tedlar® gas sampling bags, while the mixture of solid and liquid product (also called kerogen) was collected from the bottom drain valve. The reactor was rinsed multiple times using dichloromethane (DCM) solvent to collect the left-over kerogen from the impeller and reactor walls. A mildly polar solvent such as DCM is shown to act as an excellent medium to effectively separate the oil phase [24]. The kerogen was then filtered using a vacuum filtration apparatus to remove the solid particles (called bio-char). The remaining oil phase and aqueous phase were separated using a separating funnel. The DCM from

the oil phase was separated using a rotary evaporator (Heidolph Instruments), and the left-over product is termed as bio-crude.

Figure 1 a, b illustrates the temperature and pressure vs time profiles for the HTL experiments A1 to A6. In general, the experiments A3, A4, A5 and A6 with glycerol content 20, 30, 40 and 50 vol.%, respectively, took a relatively shorter time (< 80 min) to reach the final conditions compared to experiment A1 with 100 vol.% water (~ 85 min). Experiment A4 with 30 vol.% glycerol was the fastest (~ 70 min) to reach the final conditions. The average heating rate for the experiments was ~ 3.9 °C min⁻¹. During the first 30 min of heating the reactor, there was very little rise in the pressure (~ 0.06 MPa min⁻¹). After 30 min, the average rate of pressure rise for the experiments was ~ 0.33 MPa min⁻¹. The time taken to reach the final conditions is primarily influenced by the heat lost to the ambient, as well as the composition of the RDF used for the experiment. Minor change in composition in terms of the various fractions can be expected in a bulk RDF sample of 35 g used in the HTL experiments.

The mass of all the products was taken into consideration, and the typical mass balance is given by the following expression:

$$\text{Mass of (RDF + glycerol)} = \text{Mass of} \\ (\text{bio - crude} + \text{bio - char} + \text{aq. phase} + \text{gases}) \quad (1)$$

The yields of different product streams were calculated as follows:

$$\%Yield_{\text{bio-crude}} = \frac{\text{mass}_{\text{bio-crude}}}{\text{mass}_{\text{RDF}} + \text{mass}_{\text{glycerol}}} \quad (2)$$

$$\%Yield_{\text{bio-char}} = \frac{\text{mass}_{\text{bio-char}}}{\text{mass}_{\text{RDF}} + \text{mass}_{\text{glycerol}}} \quad (3)$$

$$\%Yield_{\text{aq. phase}} = \frac{\text{mass}_{\text{aq. phase}}}{\text{mass}_{\text{RDF}} + \text{mass}_{\text{glycerol}}} \quad (4)$$

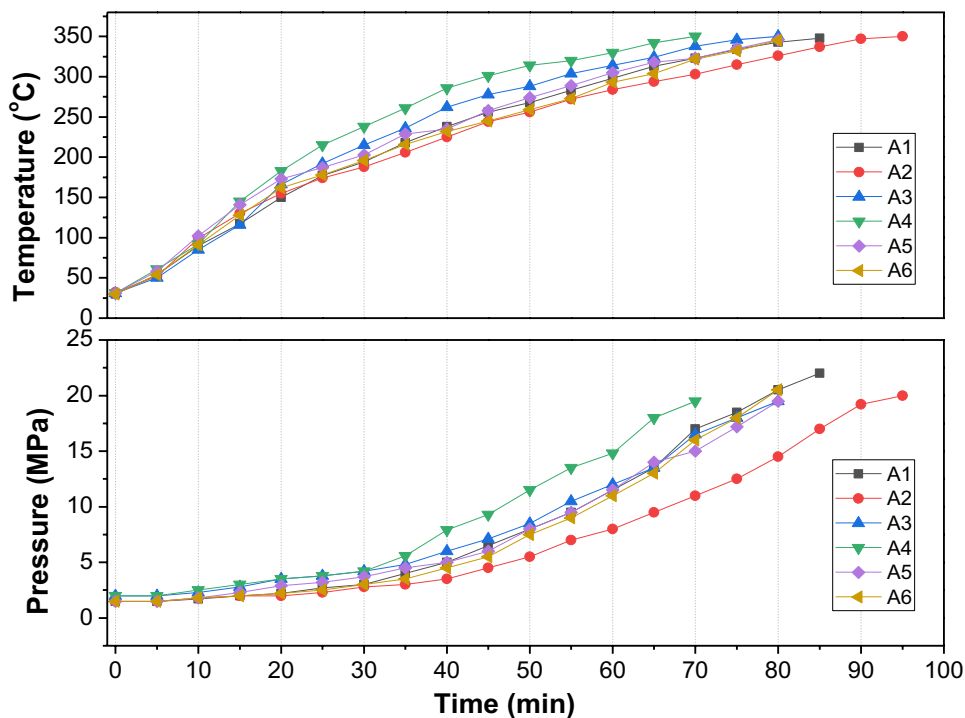
$$\%Yield_{\text{gases}} = 100 - (\text{Yield}_{\text{bio-crude}} + \text{Yield}_{\text{bio-char}} + \text{Yield}_{\text{aq. phase}}) \quad (5)$$

Since glycerol is observed to take part in the reaction under hydrothermal conditions, it is also considered in the mass balance. Interestingly, previous studies reporting the use of glycerol as a co-solvent for HTL have not considered glycerol in the mass balance and yield calculations, which might lead to the overestimation of product yields [9, 22].

2.3 Product analysis

Composition analysis of the bio-crude was performed in a gas chromatograph/mass spectrometer (GC/MS) (Shimadzu QP2020, GC/MS) equipped with a capillary column (Rxi-5Sil MS) with helium (5.5-grade purity) as carrier gas flowing through the column at a rate of 1.6 mL min⁻¹. The column oven temperature was initially maintained at 40 °C for 1 min, followed by a ramp to 300 °C at the rate of 5 °C min⁻¹ and finally held at this condition for 5 min. The

Fig. 1 (a) Temperature vs time profile for experiment A1 to A6, and (b) pressure vs time profile for experiment A1 to A6



injector temperature was set at 280 °C, and the scanning m/z range in MS was 50–500 Da. The proximate and ultimate analysis of the products were conducted as per the methods mentioned in Sect. 2.1 for characterising the feedstock. The HHVs of the RDF, bio-crude and bio-char were determined using a bomb calorimeter (IKA C2000, IKA Germany). The composition of non-condensable gases was analysed using a GC with flame ionisation and thermal conductivity detectors (GC/FID-TCD, Agilent 7820A). The gases were separated using CP Molsieve 5 Å and Porapak Q columns with ultra-high pure argon (99.995%) flowing at a rate of 10 mL min⁻¹. The FID and TCD were maintained at 260 °C and 220 °C, respectively, while the injector was set at 200 °C. The column oven was programmed at an isothermal temperature of 50 °C. The moisture present in the aqueous phase was determined using Karl Fischer titration (KF Titrino 870, Metrohm instruments). The compounds present in the aqueous phase were identified using a single quadrupole liquid chromatograph/mass spectrometer (LC/MS, Shimadzu 2020) by direct infusion method. The mobile phase used was a mixture of acetonitrile and water (25 vol. %:75 vol. %) at a flow rate of 0.6 mL min⁻¹. The oven temperature was fixed at 50 °C with an m/z scanning range between 20 and 300 Da. The ash obtained from the proximate analysis was subjected to acid digestion in a mixture of HCl and HNO₃, and the filtrate was diluted using de-ionised water. The metal ion concentration in the aqueous phase was then determined by inductively coupled plasma optical emission spectroscopy (ICP-OES) (Perkin Elmer Optima 5300 DV ICP-OES).

Energy recovery (ER) is the conversion of waste into usable heat, energy or fuel. ER for bio-crude and bio-char were calculated as:

$$ER_{bio-crude} \% = \frac{HHV_{bio-crude} * mass_{bio-crude}}{(HHV_{RDF} * mass_{RDF}) + Q_{solvents}} * 100 \tag{6}$$

$$ER_{bio-char} \% = \frac{HHV_{bio-char} * mass_{bio-char}}{(HHV_{RDF} * mass_{RDF}) + Q_{solvents}} * 100 \tag{7}$$

where $Q_{solvents} = (mC_p \Delta T)_{solvents}$, m —mass of the solvent, C_p —specific heat capacity of the solvent and ΔT =final temperature – initial temperature.

The energy recovery ratio (ERR) is defined as the ratio of output energy to input energy, and the energy conversion ratio (ECR) defined as the ratio of energy consumed to energy produced. Both ERR and ECR give valuable information on the energy efficiency of the process. The ERR and ECR for the process were calculated as:

$$ERR \% = ER_{bio-crude} \% + ER_{bio-char} \% \tag{8}$$

$$ECR \% = \frac{Energy\ required\ for\ liquefaction}{HHV_{bio-crude} * mass_{bio-crude} + HHV_{bio-char} * mass_{bio-char}} * 100 \tag{9}$$

where the energy required for liquefaction process ($E_{liquefaction}$) is determined as

$$E_{liquefaction} = \frac{mC_p \Delta T_{(solvents+feedstocks)}}{Combustion\ energy\ loss} \tag{10}$$

Here, the combustion energy loss is modestly assumed to be 0.7 [25, 26]. Carbon footprint indicates the amount of carbon dioxide released into the atmosphere. Assuming an average fuel consumption as 5 L of bio-crude for 100 km, the carbon footprint for bio-crude combustion is calculated as:

$$Carbon\ footprint\ (g_{CO_2} km^{-1}) = \frac{(A + B)}{100} \tag{11}$$

A is the mass of carbon (g) in 5 L of bio-crude, and B is the mass of oxygen (g) required for complete combustion of A. Environmental factor (E-factor) is the ratio of total waste produced from the process to the total amount of products obtained from the process. Here, the gaseous phase is considered as the waste since most of it is essentially vented out, and it contains CO₂ as the major component. E-factor is calculated as [27]:

$$E - factor = \frac{mass_{gas}}{(mass_{bio-crude} + mass_{bio-char} + mass_{aq. phase})} \tag{12}$$

Process mass intensity (PMI) is the ratio of total mass used in the process to the total mass of the useful products obtained [27]. Two different PMI values, viz., PMI⁽¹⁾ and PMI⁽²⁾, are calculated in this study as shown by the following expressions.

$$PMI^{(1)} = \frac{mass_{RDF} + mass_{glycerol} + mass_{water}}{mass_{bio-crude} + mass_{bio-char} + mass_{total\ water}} \tag{13}$$

$$PMI^{(2)} = \frac{mass_{RDF} + mass_{glycerol} + mass_{water}}{mass_{bio-crude} + mass_{bio-char}} \tag{14}$$

PMI⁽¹⁾ considers bio-crude, bio-char and the aqueous phase as valuable products, while PMI⁽²⁾ considers only bio-crude and bio-char as the valuable products. The mass of total water in Eq. (13) represents the mass of water added initially to the reactor and the water formed during the process. The aqueous phase can serve as a nutrient in algae cultivation and as a source of hydrogen through reforming process [28]. It can also be recycled in the HTL process in order to enhance the product yield in subsequent runs [29]. Owing to the abundance of N₂ and CO₂

in the gas phase, its energy content is usually low, and so it is considered as a waste stream.

3 Results and discussion

3.1 Effect of glycerol on product yields

It is evident from Fig. 2 that the yield of bio-crude increased with a concomitant reduction in bio-char yield with an increase in the amount of glycerol in the solvent mixture. The increase in bio-crude yield was only marginal and incremental, up to 30% addition of glycerol, while at 40% and 50% addition, a drastic increase in the yield of bio-crude was observed. The addition of glycerol shows a drastic decrease in the yield of bio-char from 60.5 wt.% (0% glycerol) to 20.4 wt.% (10% glycerol). This can be attributed, at least partially, to the solubilisation of the organic component of the RDF in glycerol phase, and the degradation by-products of glycerol. In fact, it has been shown that increased ash content inhibits the transformation of the feedstock in HTL. Hence, the solubilising effect

of glycerol on inorganics also tends to improve the yields of bio-crude [30]. In addition, this increase in yield of bio-crude agrees with previous studies on HTL of rice-straw and de-oiled yeast with glycerol as co-solvent, wherein the highest yields were reported with 1:0 and 1:1 ratio of glycerol:water, respectively [9, 25]. Demirbas [31], in his liquefaction study of poplar wood, stated that glycerol as a solvent reduces the surface tension of the cooking liquor at high temperatures. When glycerol initially encounters the biomass, it straightens the cellulose chains and causes swelling of the matrix. This promotes more penetration and uniform distribution of reagents within the woody biomass.

In this study, it was also observed that glycerol decomposed and reacted with the RDF and formed products that got distributed into different product phases. Earlier reports on decomposition of glycerol under HTL conditions reported the formation of acrolein as a major product, along with acetaldehyde and allyl alcohol [32]. Lehr et al. [33] have reported similar results of the formation of acrolein from glycerol in subcritical water with catalytic amounts of $ZnSO_4$. Here, the drastic increase in the yield of aqueous products provides an indication of the decomposition of glycerol at HTL conditions. Assuming Kay's rule to be valid, the pseudo-critical conditions of the water-glycerol mixture were calculated (Table 2). The heating rate and the rate of change of pressure after 30 min from the beginning of the process were determined using the temperature and pressure profiles for experiments A1 to A6 (Table 2). The experimental conditions more or less remained within the subcritical regime at all times, although the pressure exceeded the critical pressure at the end for experiments A5 and A6. This may explain the sudden jump in bio-crude yields for A5 and A6 (Fig. 2). Supercritical water is shown to improve the yield of bio-crude from lignocellulosic biomass [34]. The density and dielectric constant decrease further in supercritical water, which leads to higher diffusivity and penetration of water into the biomass matrix, thus leading to a higher degree of liquefaction.

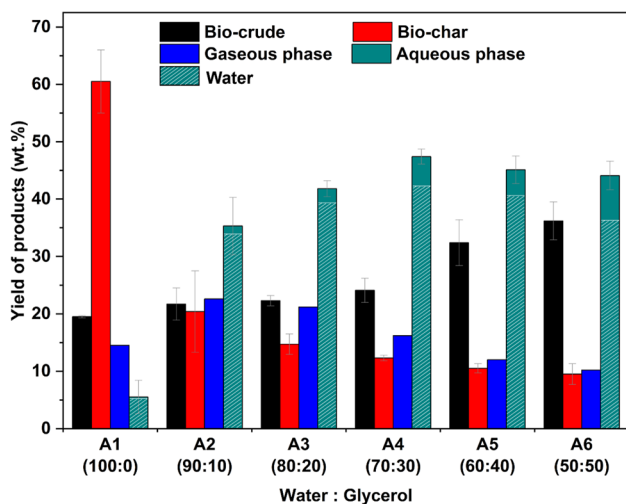


Fig. 2 Variation of product yields with different amounts of glycerol in water for a reaction temperature of 350 °C and residence time of 30 min

Table 2 Pseudocritical conditions for glycerol-water mixture along with the average heating rate and rate of change of pressure for experiments A1 to A6

Water:glycerol (vol%:vol%) (Exp. ID)	100:0 (A1)	90:10 (A2)	80:20 (A3)	70:30 (A4)	60:40 (A5)	50:50 (A6)
T_c (°C)	373.9	379.3	385.7	393.3	402.6	414.1
P_c (MPa)	22.06	21.68	20.78	19.96	18.95	17.7
Average heating rate (°C min ⁻¹)	3.7	3.3	4	4.6	3.9	3.9
Rate of change of pressure after 30 min (MPa min ⁻¹)	0.35	0.26	0.31	0.38	0.32	0.35

3.2 Properties and composition of bio-crude

The bio-crude is a viscous oily product, which appeared brownish to black in colour. The viscosity was physically observed to increase with the increase in concentration of glycerol in the mixture. The organics in the bio-crude were grouped into major functional group categories, which are depicted in Fig. 3. It is evident that the selectivity to phenols and aromatic non-phenols, which also included some oxygenated aromatics, increased with the amount of glycerol in the solvent mixture. On the contrary, the amount of aliphatic hydrocarbons was more when only distilled water was used as the solvent, and this decreased in the presence of glycerol. The aliphatic compounds included straight-chain and cyclic alkanes and alkenes ranging from C₈ to C₁₉. It is known that aliphatic compounds are formed by the decarboxylation of fatty acids formed from the hydrolysis of lipids and other organic acids. Polyethylene (PE) and polypropylene (PP) are also shown to decompose under supercritical conditions to give alkanes [35]. Thus, the formation of alkanes in the bio-crude can be attributed to the severe thermal decomposition of PE and PP present in the RDF under critical conditions.

Phenol, cyclopentenone and their derivatives were the major compounds present in the bio-crude from all the experiments. Lignin present in the lignocellulosic woody or agri-residue fraction of the RDF undergoes degradation to form phenols and phenolic derivatives like methoxy and methyl phenols. The presence of a polyol solvent such as glycerol induces increased fibre liberation, thereby promoting the degradation of lignin in the feedstock [36]. Wahyudiono et al. [37] suggested that lignin undergoes dealkylation in critical water to form catechol, which subsequently undergoes decomposition to form phenol. A brief transformation scheme of lignin and the different

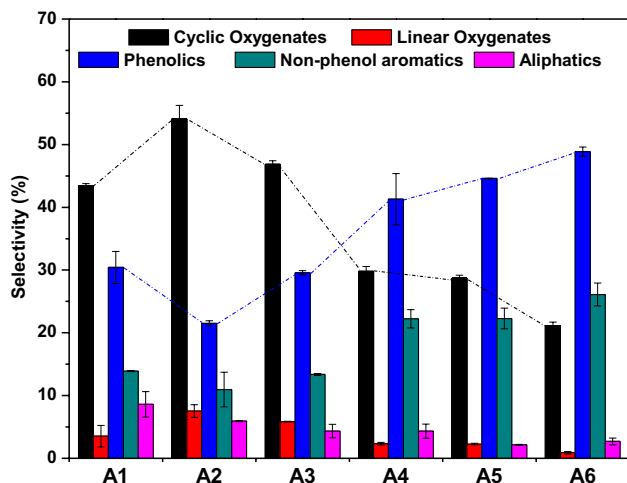


Fig. 3 GC/MS composition analysis of bio-crude from different experiments

products that can be obtained from a lignin monomer under hydrothermal conditions is presented in Fig. 4. Phenols and other aromatic compounds such as naphthalene were also the major thermal decomposition products of plastic-based components such as polystyrene and polyethylene terephthalate [38]. Generally, plastics are shown to decompose under supercritical conditions, i.e. above 400 °C, but the co-presence of reactive biomass in the feedstock and co-solvents can make the conditions milder [35, 39].

Cyclopentenones are the dehydration products of hexose and pentose sugars present in cellulosic and hemicellulosic fractions (paper and wood) of the RDF. Cellulose and hemicellulose undergo hydrolysis to form sugar monomers such as glucose, fructose, pyranose and xylose, which subsequently undergo dehydration to form furfural, furan and its derivatives. Furfural and furan derivatives undergo ring rearrangement under hydrothermal conditions to give cyclopentenones [40]. It was also reported that hydrogenolysis of 5-HMF gives dimethylfuran, which undergoes hydrolysis and condensation to form 3-methylcyclopent-2-en-1-one [41]. Cyclopent-2-en-1-one is highly valuable because of its anti-cancer activity mediated by its cyclopentenone chemical moiety [42]. The transformation pathway of carbohydrates to form cyclopentenones is illustrated in Fig. 4. In a study on HTL of woody biomass, it was observed that cyclopentenone yield generally exhibited a linear dependency on the composition of carbohydrates and lignin present in the feedstock. The cyclopentenone yield decreased as the amount of lignin increased in the feedstock [43].

Interestingly, it is observed that the selectivity to cyclic oxygenates, linear oxygenates and aliphatics decreased with glycerol addition, while the selectivity to phenolics and aromatics increased. This indicates that glycerol promotes bimolecular condensation of the cyclic and linear oxygenates with other low molecular weight oxygenates to form aromatics and phenols. In addition to this, acrolein and acetaldehyde from glycerol are shown to form aromatics and phenols by aldol condensation under liquefaction conditions [44]. Plastics with aromatic structures such as polycarbonate (PC), polyethylene terephthalate (PET) and polystyrene (PS) degrade under critical conditions to form aromatic compounds such as bisphenol-A, benzoic acid and alkyl-substituted benzenes (Fig. 4) [35]. An increase in aromatic compounds with glycerol addition indicates that glycerol also promoted the degradation of such plastics at subcritical conditions, which otherwise require supercritical conditions (> 400 °C) [35]. The selectivity towards linear oxygenates in the bio-crude was as low as ~0.9% with 50 vol.% glycerol. Mahesh et al. [22] explained that the decrease in selectivity to linear oxygenates with glycerol addition at 350 °C is due to their secondary transformation to form phenols via

Fig. 4 Transformation pathways for lignin, carbohydrates and plastics under hydrothermal conditions

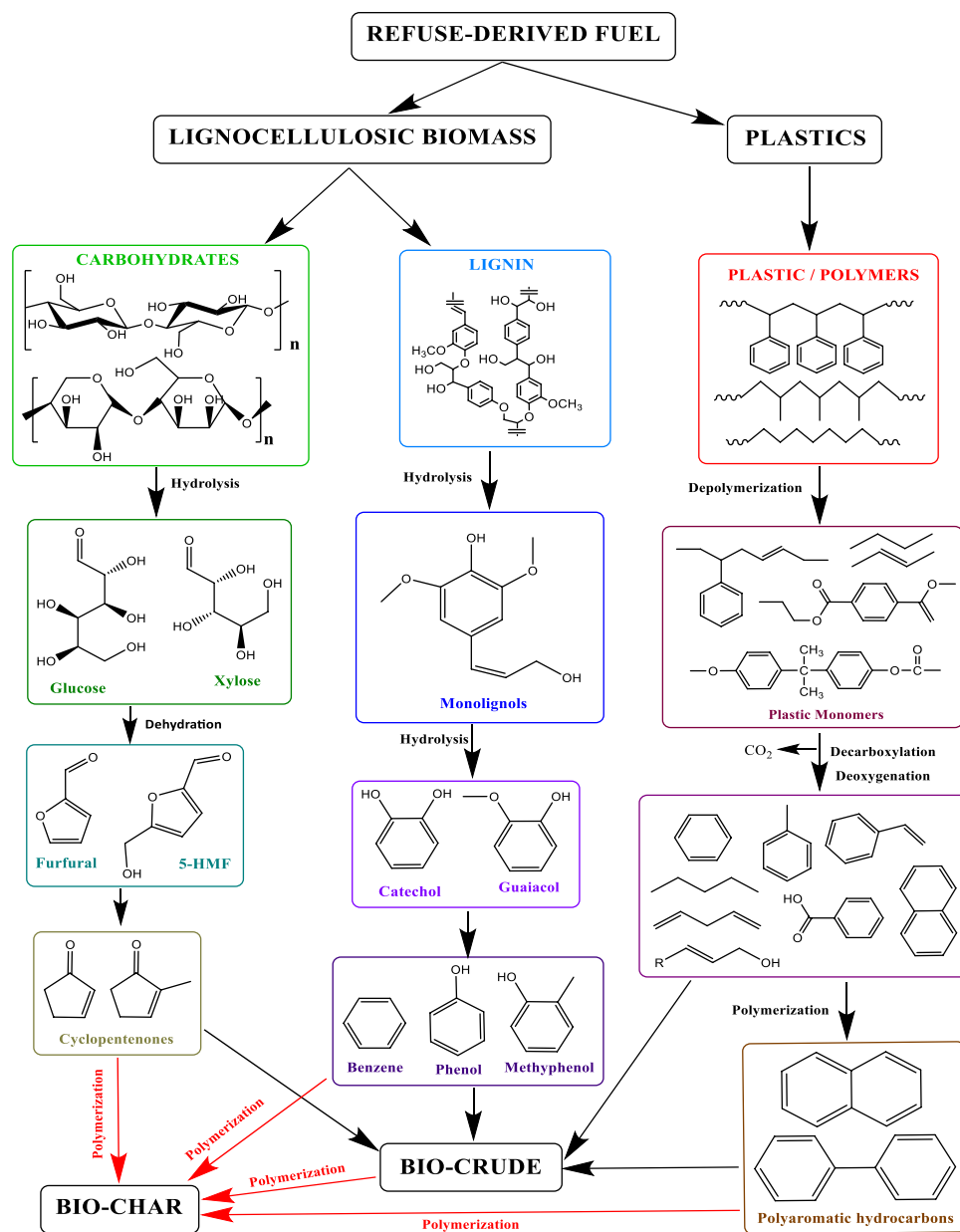


Table 3 Higher heating value and elemental composition of bio-crude

Exp.no	Water:glycerol (vol%:vol%)	HHV (MJ kg ⁻¹)	Carbon (wt% db)	Hydrogen (wt% db)	Nitrogen (wt% db)	Sulphur (wt% db)	Oxygen* (wt% db)
A1	100:0	28.8	76.6 ± 6	8.7 ± 2	0.4 ± 0.2	0	14.3
A2	90:10	28.5	76.8 ± 1	9.1 ± 0.1	0.8 ± 0.1	0.6 ± 0.1	12.7
A3	80:20	29.1	76.8 ± 1	9.1	0.6	0.3	13.2
A4	70:30	30.6	76.2 ± 1	8.8 ± 0.1	0.4 ± 0.1	0.1 ± 0.1	14.5
A5	60:40	30.7	76 ± 1	8.6	0.3 ± 0.1	0.1 ± 0.1	15
A6	50:50	30.9	79.7 ± 2	8.6	0.5 ± 0.1	0.15 ± 0.1	11.05

*O = 100 - (%C + %H + %N + %S)

cyclisation reactions. Table 3 shows the HHV and elemental composition of bio-crude.

A marginal increase in the carbon content and decrease in the oxygen content was observed as the amount of glycerol increased. In fact, Madsen et al. [45] proposed that Schiff bases formed through Maillard reactions between carbohydrates and proteins are the main reason for decreased oxygen content in the bio-crude obtained from biomass mixtures. The HHV of bio-crude increased with an increase in glycerol proportion in the co-solvent, which can be related to the comparatively lower amount of oxygen (~ 11 wt.%). Cao et al. [9] reported an increase in the carbon and hydrogen content of the heavy oil fraction by ~ 5.3 wt.% and ~ 1.1 wt.%, respectively, with an HHV of ~ 31.8 MJ kg⁻¹ when the glycerol content was increased to 50 vol.%. The HHV of the bio-crude is lesser than that of petroleum crude, owing to the presence of oxygen, which can be rectified by downstream processes like reforming and hydrocracking. The amount of nitrogen and sulphur in the bio-crude showed no particular trend as the glycerol was added as co-solvent, which is due, at least partially, to the heterogeneous nature of the feedstock.

3.3 Composition of bio-char

The bio-char obtained was dried overnight at 50 °C in an oven to remove the residual DCM solvent. The amount of bio-char formed is positively correlated to the amount of lignin and carbohydrates in the feedstock. Phenoxy radicals that are formed by thermal decomposition of lignin above 250 °C tend to undergo condensation and repolymerisation to form the solid residue [31]. Miao et al. [46] stated that the presence of proteins in high amount enhances Maillard

reaction, which tends to prevent char formation via resinification or polymerisation of furan derivatives by protecting glucose from decomposing to furan derivatives. Similarly, the presence of fatty acids in the feedstock will decrease the yield of bio-char; a binary feedstock of glucose–linoleic acid led to a decrease in the bio-char yield by four times, while the binary feedstock of guaiacol–linoleic acid completely eliminated the formation of bio-char [47].

Bio-char also contains high molecular weight polymers, insoluble fractions from the feedstock and inorganic ash. The proximate analysis and HHV of the bio-char are given in Table 4. The volatile matter of the bio-char was the highest for experiment A5, while the ash content was the least for experiment A6. It was reported that hydrothermal processing of RDF at 275 °C led to a carbon-rich hydrochar with a volatile content of 80.6 wt.% and HHV of 28.1 MJ kg⁻¹ [20]. The HHV of the bio-char increased as the concentration of glycerol increased. This can be attributed, at least partially, to the fact that the addition of glycerol might solubilise the inorganic components like hydroxides, carbonates and bicarbonates of sodium, potassium and calcium at sub-critical conditions, which leads to a net decrease in the amount of ash content in the bio-char. This eventually leads to an increase in its HHV. Bio-char from experiment A6 with 50% glycerol exhibited the lowest ash content (10.9 wt.%) and the highest HHV (31.9 MJ kg⁻¹).

3.4 Composition of gas phase

CO₂ was the major non-condensable gas formed from the HTL of RDF. The evolution of CO₂, CO and low molecular weight hydrocarbons from RDF under supercritical conditions has been previously reported in the literature [48].

Table 4 Proximate analysis of bio-char and its higher heating value

Exp. no	Water:glycerol (vol%:vol%)	Volatiles (wt% db)	Fixed carbon (wt% db)	Ash (wt% db)	HHV (MJ/kg)
A1	100:0	74.3±0.5	3.2±1	22.5±1.2	24.4
A2	90:10	76.1±0.5	2.1±2	21.8±1.9	24.4
A3	80:20	77.1±1.4	5.5±1.5	17.4±0.1	27.6
A4	70:30	78.3±2.5	9.9±0.8	11.8±1	27.8
A5	60:40	79±0.1	7.6±0.2	13.4±1	31.5
A6	50:50	75.3±0.5	13.8±0.5	10.9±0.7	31.9

Table 5 Composition of non-condensable gases (in vol.%) from different experiments

Exp. no	A1	A2	A3	A4	A5	A6
CO ₂	16.6	16.9	20.7	28.1	28.1	37.5
H ₂	0.4	0.4	1.7	0.2	0.2	5.8
N ₂	68.7	66.6	65.5	58.8	59.3	50.7
CO+light HC	12.8	15.5	11.1	4.1	3.2	4.6
CH ₄	0.3	0.4	0.7	0.02	0.6	0.07

From Table 5, it is evident that the concentration of CO₂ was the least from experiment A1, and it increased with the amount of glycerol in the solvent mixture. This could be attributed to the predominance of decarboxylation reaction during HTL. A concomitant decrease in the production of light hydrocarbons was also observed, which shows that glycerol assists in the complete degradation and depolymerisation of the organic matter in RDF. Since N₂ was used for pressurising the reactor, its concentration in the gas phase is very high. A significant amount of H₂ (5.8%) was detected from experiment A6 (50% glycerol), which is clearly due to the recombination of hydrogen-free radicals generated from the hydrogen donor solvent such as glycerol under hydrothermal conditions [22]. Trace amounts of CH₄ (< 1%) were also observed from experiments A1 to A6.

3.5 Analysis of aqueous phase

The water content in the aqueous phase from HTL experiments is provided in Fig. 2. The percentage of water in the aqueous phase decreased with glycerol addition, i.e. the amount of organics and inorganics in the aqueous phase increased with glycerol addition. The mass of water in the aqueous phase was more than the initial mass of water used as solvent for the experiment, indicating that dehydration was prevalent during the HTL process. This could be due to dehydration of the organic component of the RDF as well as that of glycerol. Water is also formed as a by-product of glycerol decomposition into acrolein at these conditions. Some of the plausible aqueous soluble compounds identified via LC/MS are listed in Table 6. Sugar monomers and levulinic acid derivatives were the major compounds derived from the carbohydrate units like starch and cellulose. Degradation products of lignin such as syringol and guaiacol were also detected. Xylose and acetic acid are the hydrolysis products of hemicellulose such as xylan [49].

Glycerol, under hydrothermal conditions, is shown to degrade to give acrolein, acetaldehyde and formic acid [32]. Some of the decomposition products of glycerol, such as acrolein and formic acid, were observed from experiment A2 onwards as the glycerol content increased in the solvent. In addition to this, glycerol also participates in condensation reactions to give phenolic and aromatic compounds under these conditions. Glyceryl guaiacolate, which is a highly water-soluble expectorant, formed possibly by the reaction of guaiacol with a glycerol intermediate, glycidol, was detected in the aqueous phase. Other polymerisation products such as ethyl syringoate and glucose phenylhydrazone were also observed in the aqueous phase. Compounds such as hexadecanoic acid, pyridine and other aromatic compounds, which were detected in the bio-crude, were also detected in the aqueous phase. Similar results of trace

presence of oily compounds in the aqueous phase were reported during HTL of rice straw [29].

Figure 5 shows the concentration of various metal ions present in the aqueous phase. The metals are usually found in the form of salts. It is evident that there is a substantial increase in the total amount of metals present in the aqueous phase as more glycerol is added to the system. While the variation is not steady, the data does support the earlier statement that glycerol may have a solubilising effect on inorganic compounds present in the system. Calcium is the most abundantly found metal, followed by alkali metals (Na and K) in the RDF. During incineration of urban wastes like RDF and MSW, Na⁺ and K⁺ are released as NaCl and KCl, which may even form stable sulphate salts in the presence of sulphur. At high temperatures, these salts tend to combine with the fly ash from incineration, and cause undesirable effects such as fouling, slagging, corrosion and deterioration of materials. However, as these alkali metal ions are trapped in the aqueous phase in HTL, such problems are minimal. The addition of glycerol aids this cause as well. Minimising the corrosive effects of salts may also facilitate the liquefaction using seawater or brackish water for scale-up purposes.

From Fig. 5, it is evident that metal ions with similar oxidation states show a similar trend in their concentration in the aqueous phase. The concentration of highly reactive alkali metals (K⁺ and Na⁺) in the aqueous phase decreases at first and then increases drastically as the concentration of glycerol increases above 30%. The concentration of transition and post-transition state metals (primarily with the oxidation states of +2 and +3) also followed a similar trend, while the only alkaline earth metal detected in the RDF, Ca²⁺, gradually increased with glycerol addition. In addition to the similar trends, a spike in the concentration was also observed for experiment A4 with 30% glycerol. Solubility of most salts in water generally increases with an increase in temperature, while it is mostly independent of pressure. In the case of common salt, NaCl, which is soluble in water, the temperature has little effect on its solubility. However, the solubility of NaCl increases by 15% in a water-glycerol system when the temperature is increased from 293 to 313 K [50]. Similarly, a sparingly soluble salt such as Ca(OH)₂ exhibits a high solubility as the amount of glycerol is increased in a glycerol-water mixture [51]. However, the dissociation constant of Ca(OH)₂ decreases with glycerol addition, indicating that its dissociation is limited in the water-glycerol system [51]. Voisin et al. [52] compiled the data on the solubility of inorganic salts in sub- and super-critical water as a function of density. It was observed that chloride and nitrate salts of Na, K, Mg, Ca and Li exhibited similar solubility values in critical water, irrespective of the cation. On the other hand, the solubility values of sulphate and phosphate salts were dependent on their hydration level and cation associated with the salt. For example, MgSO₄

Table 6 Major compounds identified in the aqueous phase from experiments A1 to A6 using LC/MS

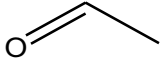
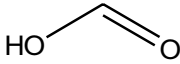
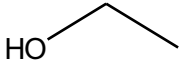

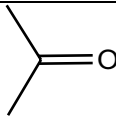
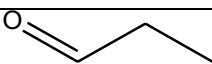
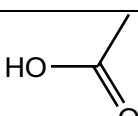
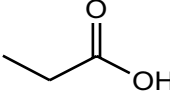
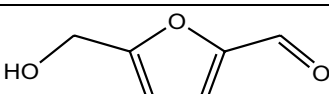
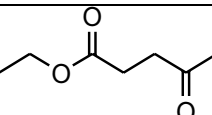
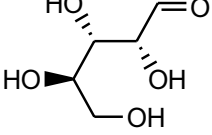
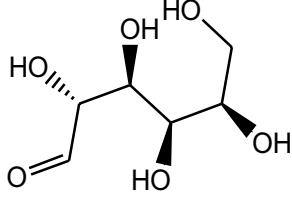
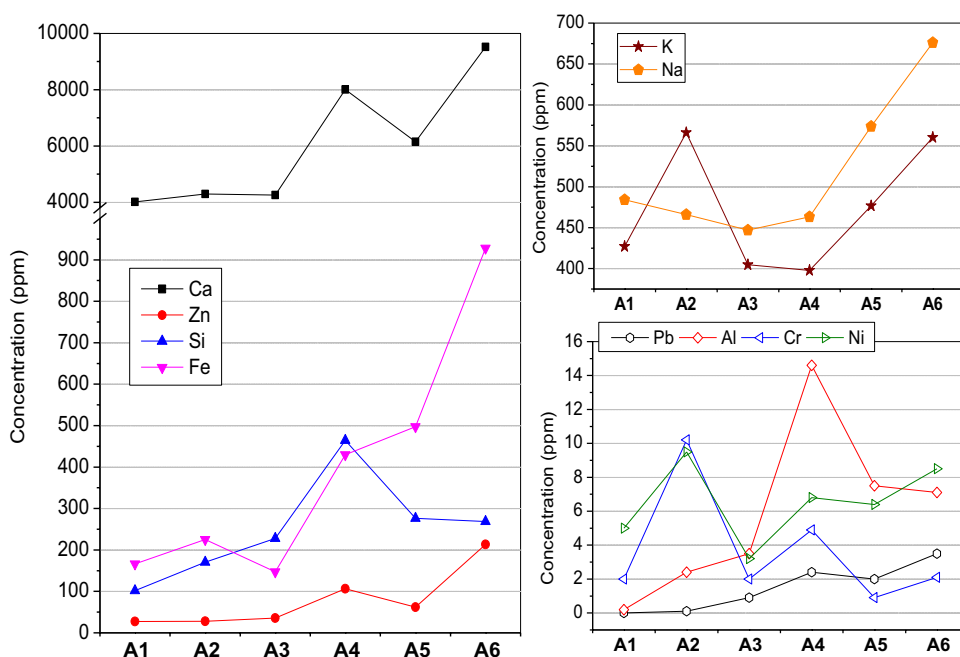
Sl. No.	Name of the compound	Molecular weight	Structure
1	Acetaldehyde	44	
2	Formic acid	46	
3	Ethanol	46	
4	Acrolein	56	
5	Acetone	58	
6	Propanal	58	
7	Acetic acid	60	
8	Propanoic acid	74	
9	Hydroxymethyl furfural	126	
10	Ethyl levulinate	144	
11	Xylose	150	
12	Hexose sugars (Glucose, Fructose)	180	

Fig. 5 Concentration of metal ions in the aqueous phase from experiments conducted at different glycerol:water ratios



was more soluble compared to Na_2SO_4 , while NaH_2PO_4 was more soluble than Na_2HPO_4 below a density of 300 kg m^{-3} [52]. In general, most metal salts show a noticeable increase in their solubility as the system approaches sub-critical and critical conditions.

3.6 Energy analysis and implications on sustainability

Table 7 shows the energy recovery (ER%) of bio-crude and bio-char, and energy recovery ratios (ERR%) for the different experiments, which were calculated using Eqs. (6–9). The gaseous and aqueous phases were excluded for the calculation of energy recovery. The ER% for bio-crude

was the least for experiment A1 (18.6%) with no glycerol and thereafter exhibited a steady increase, because the yield and HHV of bio-crude increased with glycerol addition. Conversely, the ER% for bio-char was the highest for experiment A1 (48.8%) and showed a drastic decrease as glycerol was added as a co-solvent. Although the HHV of bio-char increased, the drastic reduction in its yield led to the drop in ER%. The ERR% was the highest at 80.4% for experiment A6 with equal proportions of water-glycerol mixture. The ERR% decreased from A1 to A2, and then a steady increase in ERR% was observed as the glycerol fraction increased. This steady increase may be due to the increasing yield of the bio-crude and increasing HHV of the bio-crude and bio-char with glycerol addition.

Table 7 Energy recovery and sustainability parameters

Exp. no	Energy recovery of bio-crude (%)	Energy recovery of bio-char (%)	Energy recovery ratio (%)	Energy consumption ratio	Carbon footprint of $\text{CO}_2 \text{ km}^{-1}$	Environmental factor	PMI ⁽¹⁾	PMI ⁽²⁾
A1	18.6	48.8	67.4	2.1	120.7	0.14	1.01	13.8
A2	27.9	22.5	50.4	1.7	121	0.22	1.05	11.8
A3	32.7	20.5	53.2	1.13	121	0.21	1.07	8.9
A4	39.4	18.2	57.6	0.8	120	0.16	1.07	6.8
A5	54.9	18.3	73.2	0.5	119.8	0.12	1.06	4.6
A6	63.3	17.1	80.4	0.43	125.6	0.1	1.06	3.7
Ethanol bio-diesel (1 wt.% catalyst) [29]					-	0.3	~1.2	-
Methanol bio-diesel (1 wt.% catalyst) [29]					-	0.1	~1.1	-
Bio-crude from HTL of de-oiled yeast [25]					117	0.11	-	15
Corn bioethanol [53]					~148	-	-	-
Palm oil biodiesel [53]					~135	-	-	-

Table 7 also presents the ECR of the experiments, which were calculated using Eq. (9) and (10). An ECR value lesser than unity implies that the process is energetically feasible. From the table, it is observed that the ECR values for experiments A1, A2 and A3 are above unity, while the subsequent experiments showed ECR values lesser than 1, especially when the glycerol content is greater than or equal to 30 vol.%. This shows that 30 vol.% addition of glycerol to water is the minimum quantity required to demonstrate energetic feasibility of the process. Specific heat (C_p) of glycerol ($2.377 \text{ J g}^{-1} \text{ K}^{-1}$) is much lower than that of water ($4.186 \text{ J g}^{-1} \text{ K}^{-1}$), which leads to a decrease in the energy required for liquefaction as the amount of glycerol is increased. The decline in ECR values lower than 1.0 correlates well with the enhancement in bio-crude yield and its HHV with glycerol addition. It is important to note that the ECR value also depends on the heat lost to the environment. Higher the heat lost during the process, higher is the energy required to complete the liquefaction process. While the observations from this study show that experiments A4–A6 with glycerol are energetically feasible, it is essential to acknowledge the cost incurred in using glycerol as a co-solvent. The average global market prices of pure glycerol (~99% purity) and crude glycerol (~80–85% purity) are 1749 USD and 695 USD per metric ton, respectively [54]. High concentrations of glycerol in the solvent mixture significantly increase the operation cost during HTL. Hence, optimising the quantity of glycerol used in the HTL process is essential to ensure maximum yield and quality at a minimal operating cost. Therefore, performing a detailed techno-economic analysis using glycerol, when it is obtained as a by-product from the biodiesel industry, is worth exploring. Experiment A5 exhibited a reasonable bio-crude yield and HHV of 32.4 wt.% and 30.7 MJ kg⁻¹, respectively, along with an energy recovery of 73.2%, and an ECR value of 0.5. The organic composition and HHV of the bio-crude are similar with only minor variations when the glycerol addition to water is 30 vol.% or above. However, the variations in ERR and ECR are primarily due to the yield of bio-crude, which increases with the addition of glycerol in the solvent.

While it is important to make sure the process is feasible economically and energetically, it is essential to make sure that it leaves a positive impact on the environment. A sustainable process meets the requirements of the current generation without compromising the needs of future generations. Ideally, for a sustainable process, the impact on the environment must be less hazardous than that of fossil fuels. The green metrics or sustainability indicators required for biofuel production are carbon footprint, E-factor and PMI [27]. Table 7 shows the green metrics for HTL of RDF. The carbon footprint for bio-crude combustion measures the amount of CO₂ released to the atmosphere during bio-crude combustion. The carbon footprint due to the fossil energy

used to heat the reactor is not included in the calculation. The average carbon footprint for the bio-crude from HTL of RDF was nearly 121 g CO₂ km⁻¹, both with and without the addition of glycerol, which is almost the same value as that of gasoline (120 g CO₂ km⁻¹), but lesser than that of diesel (132 g CO₂ km⁻¹) [25]. An average *E*-factor of 0.16 indicates that the amount of waste generated from the process is lesser than the amount of valuable products produced, indicating a positive environmental impact.

PMI is entirely a mass-based green metric that determines the value of the useful products generated from a process. A value of PMI closer to unity shows that the waste generated from the process is minimum. Two PMI values are reported in this study based on whether the aqueous phase is a valuable product or not. When the aqueous phase is not considered, the PMI⁽²⁾ was found to be the highest for experiment A1, and it decreased drastically with glycerol addition, which is mainly due to the enhancement in bio-crude yield with the addition of glycerol. When all the aqueous phase products are considered, including water and organic-laden aqueous phase containing glycerol and its reaction products, the PMI⁽¹⁾ value is closer to unity for all experiments. This shows that the utilisation of the aqueous phase is very much essential to implement HTL process at a larger scale, especially in a waste biorefinery model. It is even possible to reuse or recirculate the used glycerol or glycerol-rich aqueous phase as a solvent for subsequent experiments, which can enhance the quality of the products while reducing the operational cost. The ultimate challenge in a process like this lies in wiser utilisation of all the product phases and input energy, eventually making the process more sustainable.

4 Conclusions

The effect of glycerol as co-solvent on the HTL of RDF of Indian origin was assessed in a batch reactor at 350 °C and 20 MPa. The yield and HHV of the bio-crude were maximum (36.2%, 30.9 MJ kg⁻¹) when 50:50 water:glycerol (vol.:%:vol.%) ratio was used. Mass balance of the process indicated that glycerol played an active role in the formation of the products. The addition of glycerol promoted bimolecular condensation reactions leading to a higher selectivity to phenolics and aromatic non-phenols in the bio-crude. On the other hand, the selectivity to aliphatic hydrocarbons, cyclic oxygenates and linear oxygenates decreased with glycerol addition. The major compounds in the bio-crude were cyclopentenone, phenol and their derivatives. The yield of the biochar was minimum (9.5 wt.%), while its HHV was maximum (31.9 MJ kg⁻¹) when 50:50 water:glycerol (vol.:%:vol.%) was used. The concentration of CO₂ in the gas phase increased, suggesting that the predominant mode of deoxygenation is via decarboxylation. Increasing aqueous

phase yields with glycerol addition showed the prevalence of dehydration reaction under HTL conditions. The solubilising effect of glycerol led to a significant increase in the concentration of metal ions like Ca, Fe, Zn, K, Na, Ni, Al in the aqueous phase. Low molecular oxygenates such as acetaldehyde, formic acid, ethanol along with sugar monomers were some of the organic compounds detected in the aqueous phase. From the viewpoint of energetic feasibility of the process, the minimum amount of glycerol to be added to water is 30 vol.%, which presents an ERR of 57.6%. The bio-crude obtained from experiment A4 is similar in terms of organic composition and HHV to those obtained from experiments A5 and A6, i.e. with 40 and 50 vol.% addition of glycerol. Moreover, the carbon footprint ($\sim 121 \text{ g CO}_2 \text{ km}^{-1}$), *E*-factor (~ 0.16) and PMI values make the HTL process reasonably sustainable.

Author contribution S.H.: methodology, validation, formal analysis, investigation, visualisation, writing—original draft, review and editing; P.F.P., J.N.: methodology, validation, formal analysis, visualisation; R.V.: conceptualisation, methodology, formal analysis, visualisation, writing—original draft, review and editing, resources, supervision, funding acquisition.

Funding S.H. thanks the Ministry of Education, Govt. of India, for funding the doctoral program through Prime Minister's Research Fellowship. The National Centre for Combustion Research and Development is sponsored by the Department of Science and Technology, India. The corresponding author thanks the Department of Science and Technology (DST), India, for funding the study through Waste Management Technologies Grant # DST/TDT/WMT/AgWaste/2021/15. The authors thank IIT Madras for partially funding this study through the Institute of Eminence Grant to the proposed Center of Excellence on Microgrid Technologies.

Declarations

Conflict of interest The corresponding author declares his affiliation to the start-up company M/s. X2Fuels and Energy Private Limited as a Co-founder/Director, while other authors have no conflicts of interest to declare.

References

- International Union for Conservation of Nature (2021) Marine plastic pollution. In: IUCN Issues Br. <https://www.iucn.org/resouces/issues-briefs/marine-plastic-pollution>. Accessed 30 Dec 2021
- Singh SS (2018) Government notifies new solid waste management rules. In: DownToEarth. <https://www.downtoearth.org.in/news/waste/solid-waste-management-rules-2016-53443>. Accessed 4 Oct 2021
- CPHEEO (2018) Guidelines on usage of refuse derived fuel in various industries. Central public health and environmental engineering organisation, Ministry of housing and urban affairs, Government of India
- Gerassimidou S, Velis CA, Williams PT, Komilis D (2020) Characterisation and composition identification of waste-derived fuels obtained from municipal solid waste using thermogravimetry: a review. *Waste Manag Res* 38:942–965. <https://doi.org/10.1177/07342422X20941085>
- Peterson AA, Vogel F, Lachance RP et al (2008) Thermochemical biofuel production in hydrothermal media: a review of sub- and supercritical water technologies. *Energy Environ Sci* 1:32–65. <https://doi.org/10.1039/b810100k>
- Durak H (2019) Characterization of products obtained from hydrothermal liquefaction of biomass (*Anchusa azurea*) compared to other thermochemical conversion methods. *Biomass Convers Biorefinery* 9:459–470. <https://doi.org/10.1007/s13399-019-00379-4>
- Vardon DR, Sharma BK, Scott J et al (2011) Chemical properties of biocrude oil from the hydrothermal liquefaction of *Spirulina* algae, swine manure, and digested anaerobic sludge. *Bioresour Technol* 102:8295–8303. <https://doi.org/10.1016/j.biortech.2011.06.041>
- Yin S, Tan Z (2012) Hydrothermal liquefaction of cellulose to bio-oil under acidic, neutral and alkaline conditions. *Appl Energy* 92:234–239. <https://doi.org/10.1016/j.apenergy.2011.10.041>
- Cao L, Zhang C, Hao S et al (2016) Effect of glycerol as co-solvent on yields of bio-oil from rice straw through hydrothermal liquefaction. *Bioresour Technol* 220:471–478. <https://doi.org/10.1016/j.biortech.2016.08.110>
- Nallasivam J, Francis Prashanth P, Harisankar S et al (2021) Valorization of red macroalgae biomass via hydrothermal liquefaction using homogeneous catalysts. *Bioresour Technol* 346:126515. <https://doi.org/10.1016/j.biortech.2021.126515>
- Yang W, Li X, Li Z et al (2015) Understanding low-lipid algae hydrothermal liquefaction characteristics and pathways through hydrothermal liquefaction of algal major components: crude polysaccharides, crude proteins and their binary mixtures. *Bioresour Technol* 196:99–108. <https://doi.org/10.1016/j.biortech.2015.07.020>
- Elliott DC, Schiefelbein GF (1989) Liquid hydrocarbon fuels from biomass. *Am Chem Soc Div Fuel Chem Annu Meet Prepr* 34:1160–1166. [https://doi.org/10.1016/0016-2361\(89\)90269-X](https://doi.org/10.1016/0016-2361(89)90269-X)
- Brilman DWF, Drabik N, Wądrzyk M (2017) Hydrothermal co-liquefaction of microalgae, wood, and sugar beet pulp. *Biomass Convers Biorefinery* 7:445–454. <https://doi.org/10.1007/s13399-017-0241-2>
- Wu X, Liang J, Wu Y et al (2017) Co-liquefaction of microalgae and polypropylene in sub-/super-critical water. *RSC Adv* 7:13768–13776. <https://doi.org/10.1039/c7ra01030c>
- Li L, Huang J, Almutairi AW et al (2021) Integrated approach for enhanced bio-oil recovery from disposed face masks through co-hydrothermal liquefaction with *Spirulina platensis* grown in wastewater. *Biomass Convers Biorefinery* 1:1–12. <https://doi.org/10.1007/s13399-021-01891-2>
- Xiu S, Shahbazi A, Shirley V et al (2010) Effectiveness and mechanisms of crude glycerol on the biofuel production from swine manure through hydrothermal pyrolysis. *J Anal Appl Pyrolysis* 87:194–198. <https://doi.org/10.1016/j.jaap.2009.12.002>
- Global Glycerin Market to Reach \$3.4 Billion by 2026. <https://www.prnewswire.com/news-releases/global-glycerin-market-to-reach-3-4-billion-by-2026--301494088.html>. Accessed 8 Mar 2022
- MoEF&CC (2016) Solid waste management rules. Ministry of Environment, Forest and Climate Change, Government of India
- Silva RB, Fragoso R, Sanches C et al (2014) Which chlorine ions are currently being quantified as total chlorine on solid alternative fuels? *Fuel Process Technol* 128:61–67. <https://doi.org/10.1016/j.fuproc.2014.07.003>
- Nobre C, Alves O, Durão L et al (2021) Characterization of hydrochar and process water from the hydrothermal carbonization of

- Refuse Derived Fuel. *Waste Manag* 120:303–313. <https://doi.org/10.1016/j.wasman.2020.11.040>
21. Okoligwe O, Radu T, Leaper MC, Wagner JL (2022) Characterization of municipal solid waste residues for hydrothermal liquefaction into liquid transportation fuels. *Waste Manag* 140:133–142. <https://doi.org/10.1016/j.wasman.2022.01.026>
 22. Mahesh D, Ahmad S, Kumar R et al (2021) Hydrothermal liquefaction of municipal solid wastes for high quality bio-crude production using glycerol as co-solvent. *Bioresour Technol* 339:125537. <https://doi.org/10.1016/j.biortech.2021.125537>
 23. Yerrayya A, Shree Vishnu AK, Shreyas S et al (2020) Hydrothermal liquefaction of rice straw using methanol as co-solvent. *Energies* 13:1–19. <https://doi.org/10.3390/en13102618>
 24. Qian L, Wang S, Savage PE (2017) Hydrothermal liquefaction of sewage sludge under isothermal and fast conditions. *Bioresour Technol* 232:27–34. <https://doi.org/10.1016/j.biortech.2017.02.017>
 25. Chopra J, Mahesh D, Yerrayya A et al (2019) Performance enhancement of hydrothermal liquefaction for strategic and sustainable valorization of de-oiled yeast biomass into green bio-crude. *J Clean Prod* 227:292–301. <https://doi.org/10.1016/j.jclepro.2019.04.147>
 26. Minowa T, Kondo T, Sudirjo DT (1998) Thermochemical liquefaction of Indonesian biomass residues. *Biomass Bioenergy* 14:517–524. [https://doi.org/10.1016/S0961-9534\(98\)00006-3](https://doi.org/10.1016/S0961-9534(98)00006-3)
 27. Martinez-Guerra E, Gude VG (2017) Assessment of sustainability indicators for biodiesel production. *Appl Sci* 7:869. <https://doi.org/10.3390/app7090869>
 28. Nallasivam J, Prashanth FP, Vinu R (2022) Hydrothermal liquefaction of biomass for the generation of value-added products. In: *Biomass, Biofuels Biochem.*, Elsevier. <https://doi.org/10.1016/B978-0-323-88511-9.00018-5>.
 29. Harisankar S, Prashanth FP, Nallasivam J et al (2021) Effects of aqueous phase recirculation on product yields and quality from hydrothermal liquefaction of rice straw. *Bioresour Technol* 342:125951. <https://doi.org/10.1016/j.biortech.2021.125951>
 30. Liu H, Chen Y, Yang H et al (2020) Conversion of high-ash microalgae through hydrothermal liquefaction. *Sustain Energy Fuels* 4:2782–2791. <https://doi.org/10.1039/c9se01114e>
 31. Demirbas A (2000) Biomass resources for energy and chemical industry. *Energy, Educ Sci Technol* 5:21–45
 32. Qadariah L, Mahfud S et al (2011) Degradation of glycerol using hydrothermal process. *Bioresour Technol* 102:9267–9271. <https://doi.org/10.1016/j.biortech.2011.06.066>
 33. Lehr V, Sarlea M, Ott L, Vogel H (2007) Catalytic dehydration of biomass-derived polyols in sub- and supercritical water. *Catal Today* 121:121–129. <https://doi.org/10.1016/j.cattod.2006.11.014>
 34. Chan YH, Yusup S, Quitain AT et al (2014) Bio-oil production from oil palm biomass via subcritical and supercritical hydrothermal liquefaction. *J Supercrit Fluids* 95:407–412. <https://doi.org/10.1016/j.supflu.2014.10.014>
 35. Seshasayee MS, Savage PE (2020) Oil from plastic via hydrothermal liquefaction: production and characterization. *Appl Energy* 278:115673. <https://doi.org/10.1016/j.apenergy.2020.115673>
 36. Demirbas A (2008) Liquefaction of biomass using glycerol. *Energy Sources, Part A Recover Util Environ Eff* 30:1120–1126. <https://doi.org/10.1080/15567030601100654>
 37. Wahyudiono SM, Goto M (2008) Recovery of phenolic compounds through the decomposition of lignin in near and supercritical water. *Chem Eng Process Process Intensif* 47:1609–1619. <https://doi.org/10.1016/j.cep.2007.09.001>
 38. Singh B, Sharma N (2008) Mechanistic implications of plastic degradation. *Polym Degrad Stab* 93:561–584. <https://doi.org/10.1016/j.polymdegradstab.2007.11.008>
 39. Pei X, Yuan X, Zeng G et al (2012) Co-liquefaction of microalgae and synthetic polymer mixture in sub- and supercritical ethanol. *Fuel Process Technol* 93:35–44. <https://doi.org/10.1016/j.fuproc.2011.09.010>
 40. Hao N, Alper K, Patel H et al (2020) One-step transformation of biomass to fuel precursors using a bi-functional combination of Pd/C and water tolerant Lewis acid. *Fuel* 277:118200. <https://doi.org/10.1016/j.fuel.2020.118200>
 41. Nishimura S, Ohmatsu S, Ebitani K (2019) Selective synthesis of 3-methyl-2-cyclopentenone via intramolecular aldol condensation of 2,5-hexanedione with $\Gamma\text{-Al}_2\text{O}_3/\text{AlOOH}$ nanocomposite catalyst. *Fuel Process Technol* 196:106185. <https://doi.org/10.1016/j.fuproc.2019.106185>
 42. Rosetti M, Frasnelli M, Fabbri F et al (2008) Pro-apoptotic activity of cyclopentenone in cancer cells. *Anticancer Res* 28:315–320
 43. Pedersen TH, Rosendahl LA (2015) Production of fuel range oxygenates by supercritical hydrothermal liquefaction of lignocellulosic model systems. *Biomass Bioenergy* 83:206–215. <https://doi.org/10.1016/j.biombioe.2015.09.014>
 44. Miller IJ, Saunders ER (1987) Reactions of acetaldehyde, acrolein, acetol, and related condensed compounds under cellulose liquefaction conditions. *Fuel* 66:130–135. [https://doi.org/10.1016/0016-2361\(87\)90225-0](https://doi.org/10.1016/0016-2361(87)90225-0)
 45. Madsen RB, Bernberg RZK, Biller P et al (2017) Hydrothermal co-liquefaction of biomasses-quantitative analysis of bio-crude and aqueous phase composition. *Sustain Energy Fuels* 1:789–805. <https://doi.org/10.1039/c7se00104e>
 46. Miao C, Chakraborty M, Chen S (2012) Impact of reaction conditions on the simultaneous production of polysaccharides and bio-oil from heterotrophically grown *Chlorella sorokiniana* by a unique sequential hydrothermal liquefaction process. *Bioresour Technol* 110:617–627. <https://doi.org/10.1016/j.biortech.2012.01.047>
 47. Déniel M, Haarlemmer G, Roubaud A et al (2017) Hydrothermal liquefaction of blackcurrant pomace and model molecules: understanding of reaction mechanisms. *Sustain Energy Fuels* 1:555–582. <https://doi.org/10.1039/c6se00065g>
 48. Yildirim E, Onwudili JA, Williams PT (2017) Catalytic supercritical water gasification of refuse derived fuel for high energy content fuel gas. *Waste and Biomass Valorization* 8:359–367. <https://doi.org/10.1007/s12649-016-9597-y>
 49. Phaiboonsilpa N, Champreda V, Laosiripojana N (2020) Comparative study on liquefaction behaviors of xylan hemicellulose as treated by different hydrothermal methods. *Energy Rep* 6:714–718. <https://doi.org/10.1016/j.egy.2019.11.143>
 50. Velez AR, Mufari JR, Rovetto LJ (2019) Sodium salts solubility in ternary glycerol+water+alcohol mixtures present in purification process of crude glycerol from the biodiesel industry. *Fluid Phase Equilib* 497:55–63. <https://doi.org/10.1016/j.fluid.2019.05.023>
 51. Puranik S (2020) Solubility of $\text{Ca}(\text{OH})_2$ in glycerol-water solutions at various temperatures. *Int J Grid Distrib Comput* 13:28–34
 52. Voisin T, Erriguible A, Ballenghien D et al (2017) Solubility of inorganic salts in sub- and supercritical hydrothermal environment: application to SCWO processes. *J Supercrit Fluids* 120:18–31. <https://doi.org/10.1016/j.supflu.2016.09.020>
 53. Johnson E, Heinen R (2008) Carbon footprints of biofuels & petrofuels. *Ind Biotechnol* 4:257–261. <https://doi.org/10.1089/ind.2008.4.257>
 54. ChemAnalyst (2021) Glycerine price trend and forecast. In: *ChemAnalyst*. <https://www.chemanalyst.com/Pricing-data/glycerine-1168>. Accessed 2 Jan 2022